the plant journal

SEB SOCIETY FOR EXPERIMENTAL BIOLOGY

The Plant Journal (2020) doi: 10.1111/tpj.14665

Sieve elements rapidly develop 'nacreous walls' following injury – a common wounding response?

Jan Knoblauch, Michael Knoblauch*, Viktoriya V. Vasina and Winfried S. Peters
School of Biological Sciences, Washington State University, PO Box 644236, Pullman, WA 99164, USA

Received 30 September 2019; revised 19 November 2019; accepted 9 December 2019.
*For correspondence (e-mail knoblauch@wsu.edu).

SUMMARY

Thick glistening cell walls occur in sieve tubes of all major land plant taxa. Historically, these 'nacreous walls' have been considered a diagnostic feature of sieve elements; they represent a conundrum, though, in the context of the widely accepted pressure–flow theory as they severely constrict sieve tubes. We employed the cucurbit *Gerrardanthus macrorhizus* as a model to study nacreous walls in sieve elements by standard and *in situ* confocal microscopy and electron microscopy, focusing on changes in functional sieve tubes that occur when prepared for microscopic observation. Over 90% of sieve elements in tissue sections processed for microscopy by standard methods exhibit nacreous walls. Sieve elements in whole, live plants that were actively transporting as shown by phloem-mobile tracers, lacked nacreous walls and exhibited open lumina of circular cross-sections instead, an appropriate structure for Münch-type mass flow of the cell contents. Puncturing of transporting sieve elements with micropipettes triggered the rapid (<1 min) development of nacreous walls that occluded the cell lumen almost completely. We conclude that nacreous walls are preparation artefacts rather than structural features of transporting sieve elements. Nacreous walls in land plants resemble the reversibly swellable walls found in various algae, suggesting that they may function in turgor buffering, the amelioration of osmotic stress, wounding-induced sieve tube occlusion, and possibly local defence responses of the phloem.

Keywords: cell wall swelling, *Gerrardanthus macrorhizus*, *in situ* microscopy, nacreous wall, phloem transport, pressure–flow theory, sieve tube occlusion, wounding response.

INTRODUCTION

The phloem has an essential function in the long-distance transport of photoassimilates and other materials throughout the plant body (Evert, 1982; Lough and Lucas, 2006; Knoblauch and Peters, 2013; Savage *et al.*, 2016). Phloem transport occurs as osmotically driven mass flow in symplasmically continuous pipes, the sieve tubes (Münch, 1930; de Schepper *et al.*, 2013; Knoblauch and Peters, 2017b). These tubes consist of sieve elements, elongated cells characterized by sieve plates, the perforated cross-walls between them (Esau, 1969; Behnke and Sjölund, 1990).

Despite the phloem's physiological importance, the structure of the transporting cells in their functional state and the regulation of transport rates in different parts of the plant body are still poorly understood (Knoblauch and Peters, 2010). For example, one would expect that tubular cells specialized to allow rapid bulk flow of their contents should minimize their internal hydraulic resistance. In line with this expectation, developing sieve elements degrade several organelles including their nuclei and vacuoles (Esau, 1969; Heo *et al.*, 2017), while the remaining structures are fixed in the cell periphery by minute clamps (Ehlers *et al.*, 2000; Froelich *et al.*, 2011). By contrast, sieve elements have been known since the 19th century for their often strongly thickened longitudinal walls (Esau's reviews of 1939 and 1969 provide detailed overviews of the historical literature). In some cases, for instance members of the grass family (Poaceae) such as maize, the characteristic wall thickening is restricted to sieve elements at certain positions in the vascular bundles, and remains modest and hard to identify by light microscopy alone (Evert *et al.*, 1978). In other taxa, the walls can be thickened to the point of almost complete occlusion of the sieve tubes (for example Esau and Cheadle, 1958; Evert and Eichhorn, 1976; Kuo, 1983; Evert, 1990; Nii *et al.*, 1994; for the taxonomic distribution of the phenomenon, see Table S1). Such thickenings appear due to the addition of a bulky inner wall layer that is clearly distinguished from the much denser

outer layer (Esau, 1969). Pit fields are not covered by the added wall material, so that pit channels in the thickened walls remain (Esau and Cheadle, 1958). Due to the glistening appearance of the thick inner layer in the light microscope, these strongly thickened walls have been referred to as nacré or nacreous walls (Esau, 1939). Nacreous walls decrease the cross-sectional area of the open lumen in the sieve tube and therefore present a 'feature that would seem to interfere with a free flow of materials through the sieve elements' (Esau and Cheadle, 1958, p. 546). To date, this interference has not been evaluated quantitatively.

Possible biological function(s) of sieve tube constriction by nacreous walls remain obscure. Bourquin *et al.* (2002) implied that nacreous walls helped to withstand high turgor pressure within conductive phloem tubes. However, sieve tubes generally are embedded within turgescent cells mixed with sclerenchymatic elements such as phloem fibres (Esau, 1969), which together should be sufficient to contain the turgor-driven expansion of sieve tubes. Therefore it seems implausible that sieve elements should have to constrict the pathway for assimilate transport by thickening their walls to withstand turgor. De Marco *et al.* (2016) asserted that Ca^{2+} influx into sieve elements caused cell wall thickening in phytoplasma-infected plants but provided neither quantitative data on cell wall thickness nor experimental evidence for an involvement of Ca^{2+}. In chrysanthemum, the occurrence of nacreous sieve elements or, as Israel *et al.* (1992) called them, hypertrophied sieve tube elements with abnormal wall thickenings, seemed to correlate with the symptoms of Chrysanthemum Phloem Necrosis (CPN). It seems that the intriguing possibility of a role for nacreous walls in defence responses to pathogens and pests has not been further evaluated.

Several lines of evidence suggest hydration-dependent swelling in nacreous walls. Earlier reports often described nacreous walls as thinner in ageing sieve elements and assumed this decrease in volume to be due to dehydration of the wall material (Esau, 1939, 1969). This interpretation seemed in line with the thinning of nacreous walls that were fixed for microscopy by procedures that involved dehydration (Chang, 1935; Esau, 1938), although this preparation artefact was not always observed (Cheadle and Esau, 1958; Mehta and Spanner, 1962). Hydration-induced volume changes of nacreous walls were described by Schmidt (1917), who observed pronounced swelling responses upon treatment with weak acids and certain dyes. A particularly strong swelling of the inner layer of the longitudinal walls of sieve elements was reported from *Gerrardanthus grandiflorus* (Cucurbitaceae) and several of its relatives (Zimmermann, 1922). The swelling, which occurred when tissue samples were prepared for microscopy, was so intense that, in severed sieve elements, the inner wall layer detached from the outer one and produced a filament of wall material that protruded from the cut. It is unclear whether Zimmermann (1922) considered these swellable wall layers nacreous walls, as he neither mentioned the term in the discussion of his findings nor cited pertinent literature. Conversely, the wall swelling effects Zimmermann (1922) depicted seem markedly similar to those found in sieve tubes of brown algae of the order Laminariales (Figure 1). In these kelps, sieve tube walls swell reversibly in response to changes in intracellular pressure (Knoblauch *et al.*, 2016b). For over a century, phycologists have documented various stages of wall swelling in kelp sieve tubes, apparently without ever noticing the underlying process (Knoblauch and Peters, 2017a). Thickened walls rather were interpreted as secondary walls indicating senescence (Schmitz and Srivastava, 1974; Schmitz, 1990), although widely ignored indirect evidence has suggested that wall swelling might be a wounding response elicited by preparation procedures for

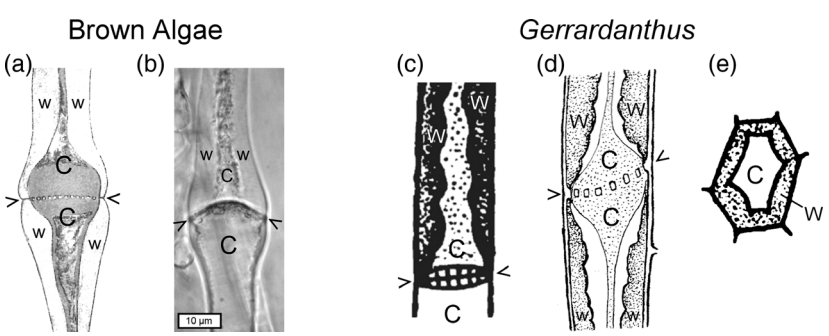

Figure 1. Published depictions of thickened lateral cell walls of sieve elements in brown algae (a, b) and *Gerrardanthus grandiflorus*, an angiosperm (c–e). Letters W and C were added to highlight thickened walls and cell contents, respectively, while arrowheads mark sieve plates. (a) Two adjacent sieve elements of *Macrocystis pyrifera* with thickened walls (Sykes, 1908, plate XIX figure 31). (b) Light micrograph of two adjacent sieve elements in *Nereocystis luetkeana*, as described by Knoblauch *et al.* (2016b). The lateral wall of the upper sieve element has swollen in response to injury, while the lower one shows the normal thin-walled habit. (c) In Zimmermann's (1922, figure 22V) sketch of two adjacent sieve elements in *G. grandiflorus*, one cell has thickened lateral walls (compare with b). (d) A more detailed drawing of two sieve elements (Zimmermann, 1922, figure 22iii) shows both cells with thickened walls. Open spaces between the collapsed cytoplasm and the thick walls indicate that the cells are wounded. The thickened inner wall layer is distinguished from the primary outer wall, which includes the sieve plate and does not contribute to wall thickening. (e) Cross-section of a sieve tube with thickened lateral wall (Zimmermann, 1922, figure 22i).

microscopy (van Went and Tammes, 1973). To date, no analogous wall swelling phenomena have been reported from land plants. However, Torode *et al.* (2018) measured gradients of elasticity across sieve tube lateral walls in the angiosperm *Miscanthus* × *giganteus*, and hypothesized that the softer inner layers of the walls might swell and shrink to buffer turgor changes, similarly as they do in kelps.

Due to the extreme sensitivity of the symplasmic sieve tube network that functions as a whole, the activities of fully functional sieve tubes can only be monitored by advanced microscopy methods in whole plants (Truernit, 2014). *In situ* microscopy is technically demanding and has been successful in a limited number of species, including *Arabidopsis thaliana* (Oparka *et al.*, 1994; Froelich *et al.*, 2011), the legume *Vicia faba* (Knoblauch and van Bel, 1998), the squash *Cucurbita maxima* (Furch *et al.*, 2010), the morning glory *Ipomoea nil* (Knoblauch *et al.*, 2016c), and the kelp *Nereocystis luetkeana* (Knoblauch *et al.*, 2016b). Vines like *I. nil* lend themselves comparatively well to *in situ* microscopy, as their flexible shoots can be mounted on microscope stages with minimal disturbance of the rest of the plant (Knoblauch *et al.*, 2016c). Therefore, we chose the vine *G. macrorhizus*, a close relative of the species that Zimmermann (1922) had worked on, to study sieve element walls with three aims in mind. First, because Zimmermann (1922) had remained silent on this point, we sought to determine whether the thickened walls in *Gerrardanthus* were 'nacreous' by commonly applied structural criteria. Second, we wished to develop a quantitative estimate of how severely wall thickening reduced the open lumen of sieve tubes in this species. Finally, we aimed at elucidating by *in situ* microscopy whether these thickened walls actually were present in transporting sieve tubes, or whether they might be functional analogues of the swellable walls of kelp sieve tubes.

RESULTS

Nacreous walls in *G. macrorhizus* sieve tubes?

We examined fresh, hand-cut cross-sections of internodes of *G. macrorhizus* with the confocal laser-scanning microscope (CLSM) using calcofluor white (CFW) and aniline blue (AB) as specific cellulose and callose stains, respectively. Vascular bundles showed the structure commonly found in eudicots, with the xylem, fascicular cambium, phloem, and a more or less developed sclerenchyma cap arranged in sequence along radial axes (Figure 2a). The phloem was characterized by cells that were partially filled by cell wall material, as indicated by cellulose-linked fluorescence (Figure 2a). We further analyzed sections taken from series of 15 internodes per shoot, starting with an internode at 5 cm from the shoot apex and extending to an internode about 60 cm from the apex. We evaluated 81 sections in total, and produced image stacks covering between 8 and 20 μm along the internode axis, i.e. perpendicular to the plane of each section. In these 81 stacks, we detected 65 sieve plates (Figure 2b, top) at distances of at least 3 μm from both the upper and lower end of the stack. Obviously, the presence of sieve plates identified sieve

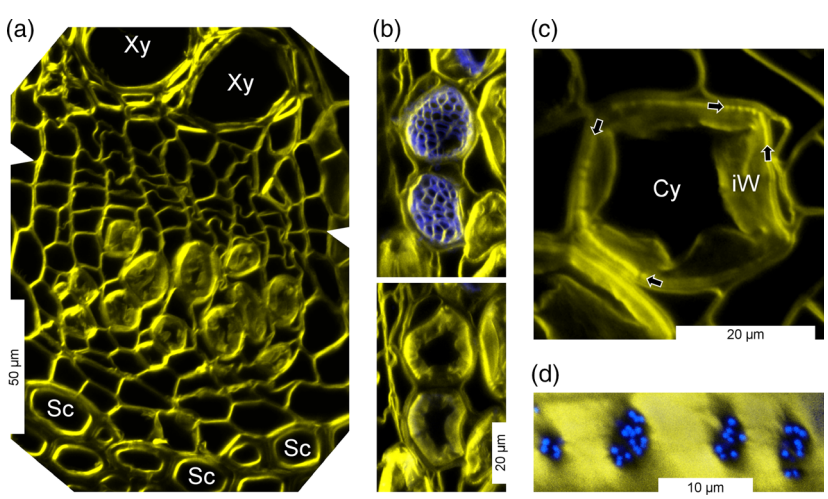

Figure 2. Sieve tube structure in internodes of *Gerrardanthus macrorhizus* (confocal laser-scanning micrographs; yellow: the cellulose marker calcofluor white (CFW); blue: the callose marker aniline blue (AB)). (a) Vascular bundle in cross-section, showing large xylem vessels (Xy) and thick-walled cells of a sclerenchyma cap (Sc). The fascicular cambium with its thin-walled cells is marked by arrowheads at the left and right edges of the image. Located between cambium and sclerenchyma, the phloem includes 12 cells partially filled with wall material of fluffy appearance. (b) The perforate structure and callose staining of sieve plates identifies sieve tubes unambiguously (top). Focusing on the same tubes just below the sieve plates (bottom) reveals a partial filling of the tubes with wall material as observed in (a). (c) Higher magnification of a sieve element indicates that the irregularly thickened inner wall layer (iW) emitting a weak cellulose signal is enclosed in a thin outer layer that fluoresces more intensely (arrows). Cy, cytoplasm of the sieve element. (d) Lateral sieve tube walls often possess rows of pits, characterized in top view by reduced cellulose-linked fluorescence and multiple discrete foci of callose-linked fluorescence.

elements. By moving up or down the image stacks from the level of each sieve plate by 3 μm or more when possible (Figure 2b, bottom), we found that the lateral walls were thickened in 60 of the 65 unambiguously identified sieve tubes (92%). Because the depth covered by our image stacks was only a fraction of the length of typical sieve elements (150−250 μm; see Figure 5 below), our count of five (8%) unambiguously identified sieve tubes without evidence for wall thickening might have included false negatives, that is, tubes that actually had thickened walls in regions not covered by the image stacks. Thus it appeared that thickened walls were a characteristic feature of sieve elements in general.

The thickening of sieve tube lateral walls was due to a bulky, geometrically irregular inner wall layer (Figure 2c). On CLSM micrographs, this inner layer was distinguishable from a thin outer layer by the intensity of the cellulose-linked fluorescence that the layers emitted, which could be explained by a lower density of cellulose fibrils in the thickened inner layer compared with the outer one (Figure 2c). Serially arranged pits in the lateral sieve element walls correlated with groups of foci of callose-linked fluorescence (Figure 2d), probably the callose collars of plasmodesmata.

The appearance of sieve elements in cross-section was essentially the same in the transmission electron microscope (TEM) as in the CLSM. A dense outer cell wall that resembled the cell walls of the neighbouring cells enclosed an irregularly thickened, less dense inner wall (Figure 3a). The higher power of TEM revealed fibrils in the thickened inner wall layer that appeared to be embedded in an unstructured matrix. These fibrils were oriented circumferentially, at a right angle with respect to the sieve tube's axis (Figure 3b).

In summary, the cell specificity and the structural as well as ultrastructural features of the thickened sieve element walls we observed in *G. macrorhizus* agreed with published characterizations of nacreous walls in general, and with the description of swellable sieve tube walls in *G. grandiflorus* (Zimmermann, 1922) in particular.

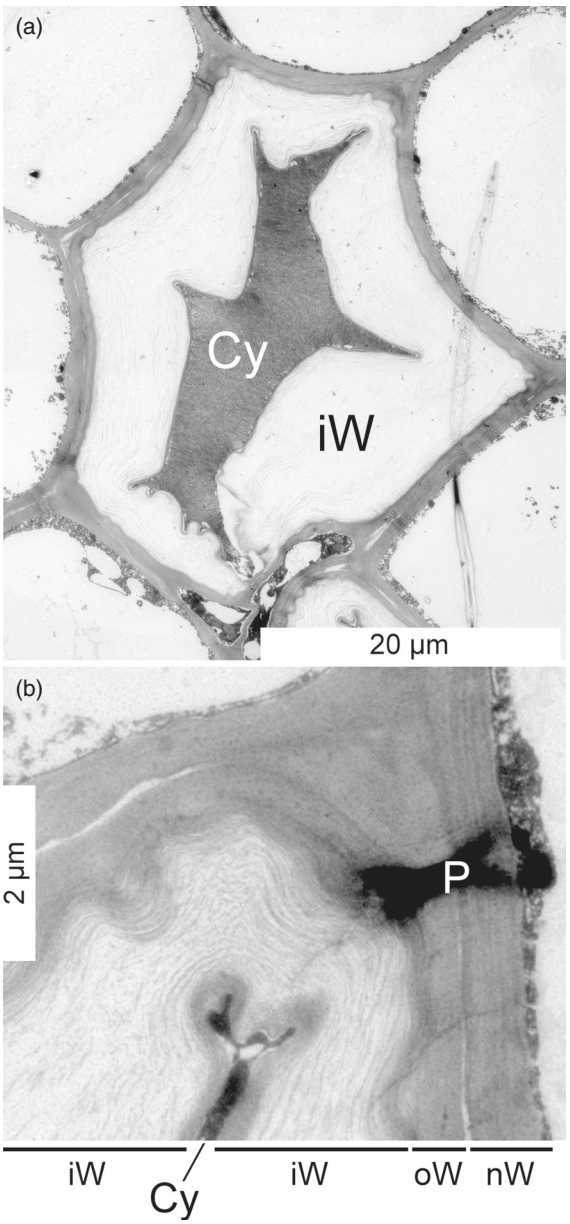

Figure 3. Transmission electron micrographs of a sieve element from an internode cross-section of *Gerrardanthus macrorhizus*. (a) The sieve element's irregularly thickened inner wall layer (iW) is weakly stained and clearly distinguished from the outer, primary wall layer, which is darker and resembles the non-thickened walls of the other cell types. The cytoplasmic space of the sieve element (Cy) is severely constricted and the cytoplasm appears condensed, unlike that of the neighbouring cells. (b) Higher magnification of a different sieve element shows the thickened inner wall (iW) as well as the outer wall (oW), which structurally resembles the walls of the neighbouring cells (nW). The inner wall consists of numerous circumferentially oriented fibrils embedded in a light matrix, but is much denser adjacent to the cytoplasmic lumen (Cy). A pit (P) sectioned in its periphery is seen between the sieve element and its parenchymal neighbour.

Constriction of the sieve tube lumen by nacreous walls

To quantify the constriction of sieve tube lumina by nacreous walls, we analyzed 150 sieve tubes on CLSM micrographs of 10 internode cross-sections, each taken from 5, 30, and 55 cm distance from the shoot apex. We first measured the area enclosed by the bright, cellulose-linked signal from the outer cell wall layer. This area is the potential open lumen (*p*OL) that would be available for transport in the absence of nacreous walls; it varied widely with a median of 181 μm^2 (Figure 4a). Next, we determined the area of the actual open lumen (*a*OL) in the same tubes and calculated the relative open lumen ($rOP = 100 \times aOL\ pOL^{-1}$) for each tube. There was no correlation of *r*OL with *p*OL ($r^2 < 0.01$; Figure 4a), implying that the degree to which nacreous walls constricted sieve tubes did not depend on sieve tube diameter. The distribution of the values of *r*OP

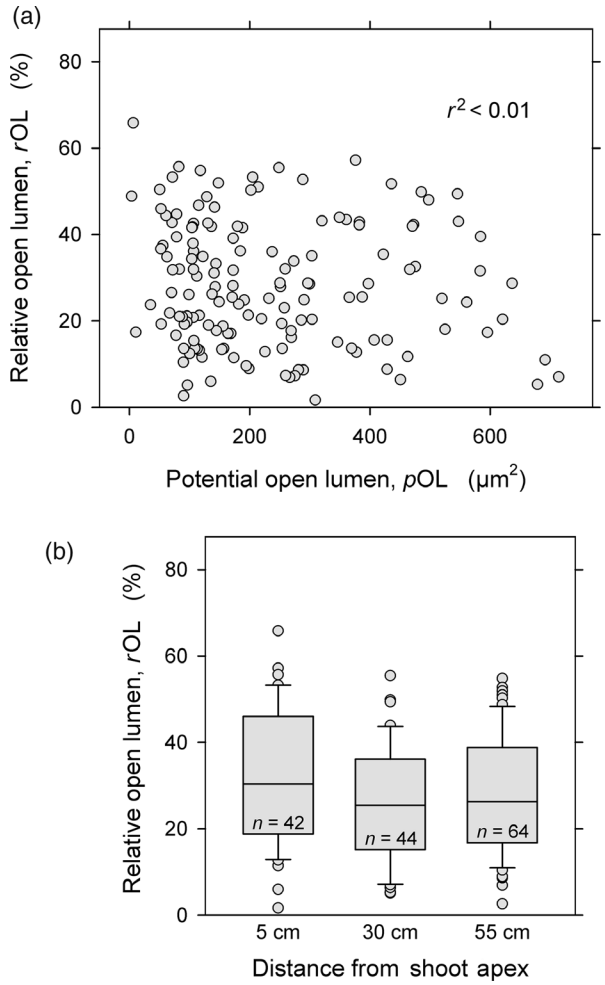

Figure 4. Analysis of the constriction of the sieve tube lumen by nacreous walls as deduced from confocal laser-scanning micrographs of cross-sections of *Gerrardanthus macrorhizus* internodes. (a) The lack of correlation between the area enclosed by the outer wall layer (potential open lumen, *p*OL) and the actual open lumen expressed as a percentage thereof (*r*OL) indicates that the degree of constriction caused by nacreous walls does not depend on tube size. (b) Distribution of *r*OL values at three distances from the shoot apex. Boxes represent the second and third quartiles, the median is indicated as a horizontal line, and whiskers reach from the 10th to the 90th percentile. The number of sieve tubes analyzed is given in each box.

were fairly uniform between the sections taken from different positions along the shoot (Figure 4b), and indicated that nacreous walls reduced the cross-sectional area of the open lumen to about one-quarter on average. Therefore, assuming that sieve elements are cylindrical tubes, flow is laminar, and the sieve tube contents are incompressible, we could apply the Hagen–Poiseuille law, according to which volumetric flow rates depend on tube diameter to the fourth power (Douglas *et al.*, 1995). Consequently, we estimated that the nacreous walls in our sample reduced flow, all other parameters being equal, by a factor of around 0.06. However, this very significant reduction would still be an underestimation of the physical effects that nacreous walls have in reality.

To see how the reduction of the cross-sectional area of the sieve element lumen by nacreous walls varied along the cell axis, we analyzed the geometry of entire sieve elements. As the preparation of phloem tissue for the microscopic observation of whole sieve elements in side view usually is more successful using leaf veins rather than internodes, we examined vascular tissues in excised leaves. Most sieve elements were 150–250 µm long (Figure 5a). Their lumina were partly occupied by the thickened, nacreous wall (Figure 5b). The remaining open lumen branched out to connect to the numerous pits in the outer wall layer (Figure 5b,c). This resulted in complex shapes of the open lumen between the irregular lobes and folds of the nacreous wall, as seen in the 3D reconstruction of a representative sieve element in Figure 5(d). The degree by which the lumina of sieve elements were constricted by nacreous walls varied significantly along the cell from sieve plate to sieve plate (70% to >99% of the cross-sectional area of the tube in Figure 5d). Therefore the constrictions seen on cross-sections placed randomly along the axes of sieve elements will almost always be less pronounced than the maximum constriction on which the reduction of overall flow rate depends.

Transporting sieve tubes lack nacreous walls

Our above findings indicated that the sieve tubes we had analyzed were efficiently occluded by nacreous walls, leaving us with two alternative conclusions. Either phloem transport in *G. macrorhizus* did not occur as symplasmic mass flow, or the sieve tubes we had studied did not represent the functional state. We tackled the problem by injecting carboxyfluorescein diacetate (CFDA), a membrane-permeant fluorescent dye, through stomata into leaves still attached to the living plant. After entering live cells, CFDA is transformed into the membrane-impermeant carboxyfluorescein (CF) by unspecific enzyme activities, and can then move between symplasmicly connected cells. CF that reaches transporting sieve tubes will be translocated, enabling the identification of active tubes through a shallow cut made in the leaf's mid vein a few centimetres downstream of the application site.

CF fluorescence in the observation window appeared within minutes after CFDA application, as expected if phloem transport occurred by mass flow. The translocated CF stained not only sieve elements but also companion cells (Figure 6), highlighting the symplasmic connectivity between the two cell types. The fluorescence signal from sieve elements, which could only have originated from the *a*OL – the actual open lumen – showed no constrictions by thickened walls. In optical sections perpendicular to the sieve tube axis, the shape of the sieve element lumina

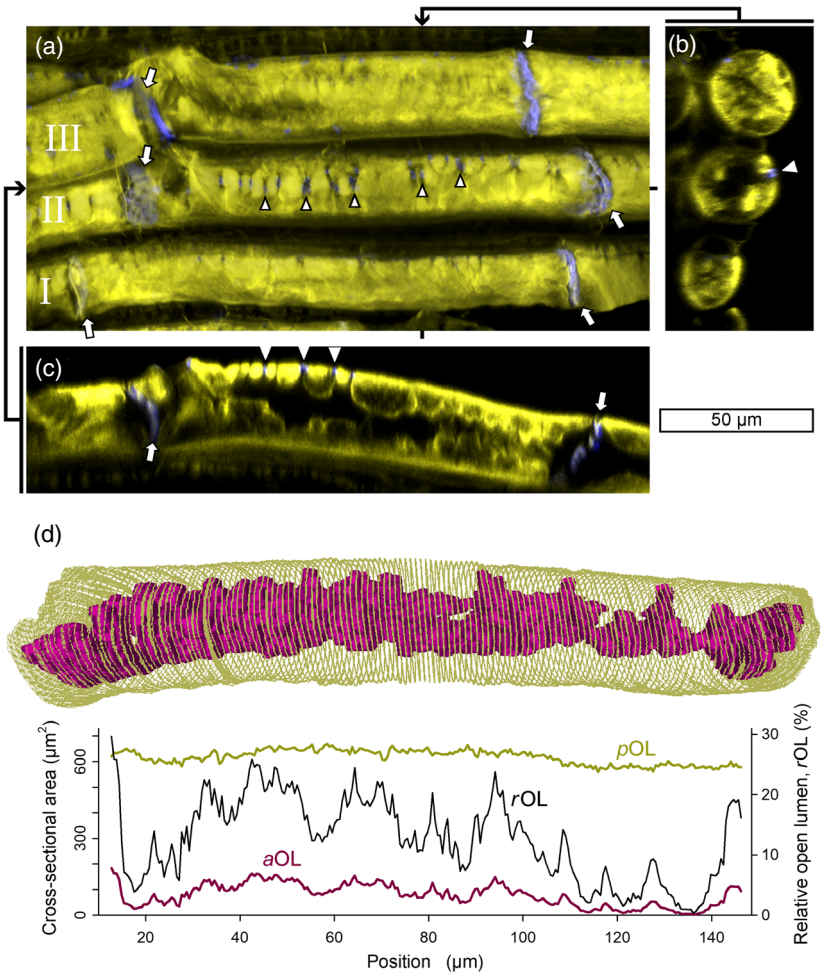

Figure 5. Variation of the degree of sieve tube occlusion by nacreous walls along the tube axis in *Gerrardanthus macrorhizus* (confocal laser-scanning micrographs; yellow: the cellulose marker calcofluor white (CFW); blue: the callose marker aniline blue (AB)). (a) Z-projection of an image stack taken of three sieve tubes (I, II, III). Cellulose appears to fill the entire tubes. Sieve plates (arrows) and pits (examples highlighted by arrowheads) exhibit callose staining (blue). (b) Optical section perpendicular to the long axis of the sieve tubes, localized at the level of one of the marked pits in tube II. Tubes are mostly filled by a material emitting cellulose-linked fluorescence. The remaining open lumen (no staining) is widest in tube II and is connected to a pit in the primary wall (arrowhead). (c) Optical section along the axis of tube II. Pits connect to the lumen (examples marked by arrowheads). (d) 3D model of the sieve element seen between sieve plates of tube II in (a) (magenta: open lumen; ochre: cell circumference). The plot below shows the cross-sectional areas enclosed by the outer wall layer (potential open lumen; *p*OL) and the actual open lumen (*a*OL) along the sieve element's axis (12 µm at each end including sieve plates are omitted). The actual open lumen is also shown as a percentage of the potential open lumen (*r*OL; ordinate on the right).

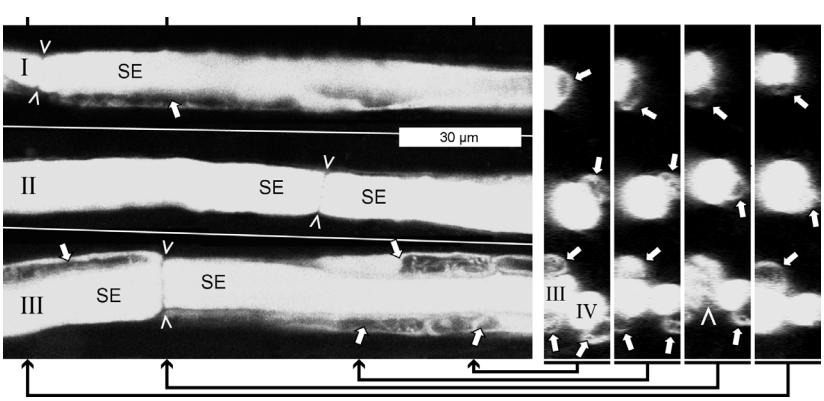

Figure 6. Transporting sieve elements in a *Gerrardanthus macrorhizus* leaf attached to the live plant. The fluorescence signal shown on these confocal laser-scanning micrographs originates from carboxyfluorescein (CF) moving with the assimilate stream. On the left, three partial images selected from different depths of a z-stack show sieve elements (SE; sieve plates located between arrowheads) of three sieve tubes (I, II, III) with neighbouring companion cells (arrows). On the four optical sections of the image stack computed for the indicated positions on the right, a fourth sieve tube (IV) is seen next to tube III. The open lumina of all sieve tubes in which CF is transported have more or less circular shapes.

always was more or less circular (Figure 6), in clear contrast with the appearance of sieve elements with nacreous walls (Figures 2, 3 and 5).

After transporting sieve tubes had been identified in fluorescence mode, we switched to bright field observation to examine the vicinity of the active sieve tubes.

We did not see any structures that resembled nacreous walls in the tissues around actively transporting tubes.

A wounding response *in situ*

The distinct structures of sieve elements in live plants (Figure 6) and in sections (Figures 2, 3 and 5) suggested that nacreous walls in *G. macrorhizus* might be a response to the wounding that inevitably occurs when tissues are sectioned. To evaluate the possibility, we wounded sieve elements transporting CF by puncturing them with micropipettes.

When an actively transporting sieve element (Figure 7a) was punctured, its CF-stained contents contracted within a minute into a thread with wavy outlines (Figure 7b). The stained lumina of adjacent sieve elements retained their circular cross-sectional shape, while that of punctured cells became point- or slit-shaped (Figure 7b). The sieve plates bordering the punctured sieve element curved toward the contracted cytoplasmic lumen (Figure 7b), indicating a pressure gradient across the plates. In adjacent sieve elements, less densely stained, flexible streaks became visible, which accumulated over time at the end of the sieve element pointing toward its punctured neighbour (Figure 7b). These structures resembled wounding-induced P-protein plugs that have been described from other species (Knoblauch and van Bel, 1998). The space formerly occupied by the lumen of a punctured sieve element became dark, not emitting any fluorescence. When we added CFW to the observation window, these dark spaces showed an irregular cellulose-linked staining of strongly varying intensity (Figure 7d). This response to CFW staining matched the behaviour of nacreous walls in sieve tube sections (Figures 2 and 5).

Taken together, our observations supported the idea of complex wounding responses in sieve tubes, including rapid swelling of inner cell wall layers following turgor loss

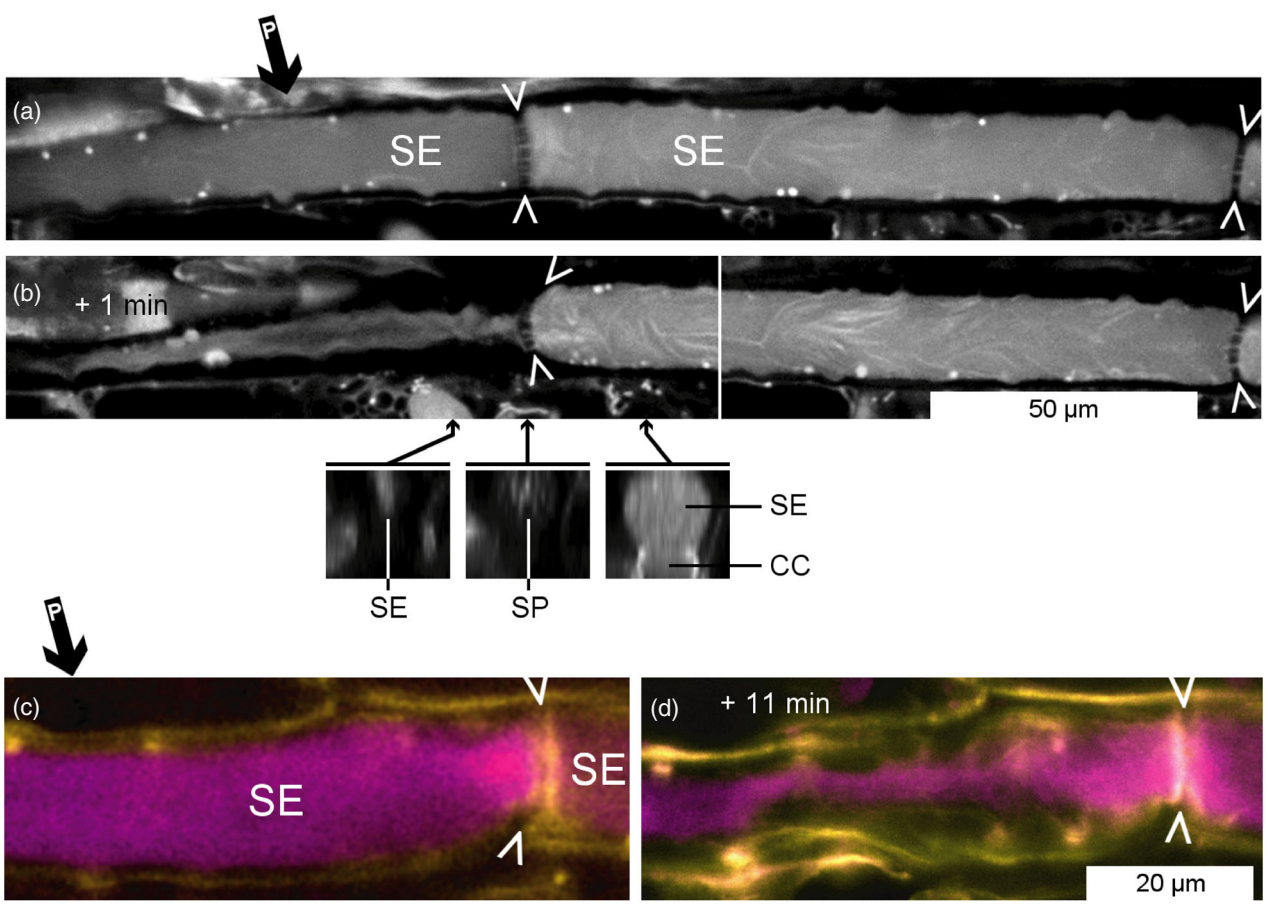

Figure 7. Wounding response of transporting sieve elements (SE) in *Gerrardanthus macrorhizus* leaves attached to the live plant. Confocal laser-scanning micrographs showing the fluorescence of the phloem-mobile carboxyfluorescein (CF) alone (a, b) or in combination with the cellulose marker, calcofluor white (CFW) (c, d; CF: magenta, CFW: yellow). (a) Transporting sieve tube just before impalement of one of the sieve elements by a micropipette (position indicated by arrow P). Individual sieve pores are resolved in the sieve plates (between arrowheads). (b) At 1 min after impalement, the lumen of the punctured cell has collapsed. The different cross-sectional shapes of the punctured and the unaffected sieve element are shown in the optical sections below (SE: sieve element, CC: companion cell, SP: sieve plate). (c) Transporting sieve tube before impalement. (d) The same cells 11 min after impalement. The space between the outer cell wall layer and the collapsed cytoplasmic compartment shows irregular cellulose-linked staining.

in injured sieve elements, combined with the formation of plugs from P-proteins and other materials in adjacent sieve elements.

DISCUSSION

Nacreous walls exist only in wounded sieve tubes

The observation of transporting sieve elements is technically demanding, as it requires *in situ* microscopy of fully functional sieve tubes in minimally disturbed, intact plants. Protocols required for this kind of observation have been developed for a limited number of species (*for example* Oparka *et al.*, 1994; Knoblauch and van Bel, 1998; Furch *et al.*, 2010; Knoblauch *et al.*, 2016b,c). In all of these species, active sieve elements essentially are open cylinders, representing a geometry optimized for mass flow of the cell contents. In none of these, nacreous walls have been observed. The adaptation with modifications of *in situ* microscopy methods enabled our key finding in *G. macrorhizus*, namely the discrepancy between the structure of sieve tubes prepared for light and electron microscopy by standard methods on one hand, and that of transporting sieve tubes in live plants on the other. Transporting sieve elements in intact *G. macrorhizus* are, in fact, open cylinders (Figure 6), very much like those previously described from other species. However, when excision of organs (as for Figure 5), sectioning of tissues (as for Figure 2), or complex fixation procedures (as for Figure 3) were involved, *G. macrorhizus* sieve tubes were mostly occluded by thickened cell wall layers that appeared equivalent to the nacreous walls discussed in the classical literature. Therefore it was evident that the nacreous walls in *G. macrorhizus* were a preparation-related wounding effect. The fact that we could induce the rapid, local formation of nacreous walls by puncturing transporting sieve elements (Figure 7) corroborated this conclusion. Most importantly, our findings implied that no micrograph of sieve tubes with nacreous walls could be considered a representation of the functional translocation system.

How far can this conclusion based on findings in *G. macrorhizus* be generalized? Nacreous walls have been reported from all major groups of vascular plants including pteridophytes (Evert and Eichhorn, 1976), gymnosperms (Sterling, 1946; Chafe and Doohan, 1972), and angiosperms (Esau, 1969), as well as from leptoids, the putatively conducting cells in mosses (Stevenson, 1977; Table S1). In many cases, published micrographs of nacreous walls in sieve elements are so similar to our images that we have no doubt about them showing the same phenomenon (for example, compare our Figure 2c with figures in Esau and Cheadle (1958); our Figure 3a with figure 35 in Kuo and Stewart (1995), figure 2 in Machado and Sajo (1996), and figure 31 in Schlag and Gal (1996); our Figure 3b with figure 4 in Cronshaw (1975), figure 8 in Israel *et al.* (1992), and figure 3 in Nii *et al.* (1994); our Figure 4c with figure 3 in Behnke (1971), figure 8 in Kuo (1983), and figure 14 in Gilliland *et al.* (1984)). On the other hand, when large numbers of species were screened systematically, nacreous walls were found in some taxa but not in others (Esau and Cheadle, 1958; Kuo, 1983; Table S1). In angiosperms, for which the most extensive information is available, the reported occurrence of thickened sieve tube walls does not correlate with phylogeny (Figure S1). Moreover, nacreous walls have been reported to occur during certain developmental stages and to shrink or disappear later in some species (Sterling, 1946; Evert, 1963; Evert and Eichhorn, 1976; Schlag and Gal, 1996), while in others they persist (Behnke, 1971; Botha and Evert, 1981; Gilliland *et al.*, 1984). Thus it may seem as if only sieve elements of certain species and at certain stages are able to respond to wounding by rapid wall thickening. However, nacreous walls so far have never been considered to potentially result from rapid wall swelling following wounding. Consequently, no efforts have ever been made to control, avoid, or specifically induce the development of nacreous walls during the preparation and fixation of specimens for microscopy. Therefore we cannot exclude that different methods of sample preparation promote or inhibit the rapid development of nacreous walls in different ways, and have contributed to the apparently patchy distribution of nacreous walls across taxa and developmental stages. Taking these aspects together, we conclude that rapid cell wall swelling leading to structures known as nacreous walls probably occurs as a wounding response in sieve elements of numerous land plants, but maybe not in all, and in a given species perhaps not at all developmental stages.

Mechanism(s) of wall swelling

In injured sieve elements, nacreous walls replace most of the cell's lumen in under 1 min (Figure 7a,b), much too fast to be explained by cell wall synthesis. In any case, wall synthesis is unlikely to be involved as mature sieve elements lack both Golgi apparatus and cytoskeleton. The Golgi apparatus is required to produce wall components other than cellulose and callose, and the cytoskeleton guides Golgi-derived vesicles along the secretory pathway (Boutté *et al.*, 2007; Carpita, 2012; Kim and Brandizzi, 2016). Nacreous wall formation rather reminds us of the similarly rapid wall swelling observed in sieve tubes of kelp (Knoblauch *et al.*, 2016b) and somatic cells of various algae (Kotte, 1915; Mostaert and King, 1993; Holzinger *et al.*, 2015). The ability of these algae to avoid plasmolysis by balancing protoplast shrinkage through wall swelling is thought to confer decisive advantages in habitats characterized by fluctuating external osmolarity (Biebl, 1938; Mostaert *et al.*, 1995; Karsten, 2012). The structure of algal swellable walls is intriguingly similar to that of nacreous walls, as both consist of a dense outer layer and an inner

layer with transversely oriented fibrils dispersed in an apparently swellable matrix (Figures 2c and 3b; Walter and Kreeb, 1970; Cronshaw, 1975; Knoblauch *et al.*, 2016b).

The mechanism(s) of rapid wall swelling responses remain elusive at this time, although technological hydrogels, complex polymers exhibiting reversible swelling linked to water uptake (Kopeček, 2007; Buwalda *et al.*, 2014), may provide functional models. If so, the tendency of the wall material to swell through water uptake should be balanced by the compressive force the turgescent protoplast exerts perpendicular to the surface of the wall. The balance between the two forces may shift depending on conditions, at least in algae including kelp in which cell wall swelling is reversible (Karsten, 2012; Knoblauch *et al.*, 2016b). In kelp, sieve tubes are embedded in a gelatinous extracellular matrix rather than in live tissues, which facilitates microscopic observation and treatments such as cell microinjection (Knoblauch *et al.*, 2016a). So far we have been unsuccessful in demonstrating reversibility of nacreous wall formation in the much more sensitive phloem tissue of vascular plants. We anticipate that further studies of sieve elements in comparatively simple systems such as kelp will help to elucidate the basic mechanism(s) of reversible wall swelling, which we expect will inform our search for the functioning of nacreous walls in vascular plants.

Possible functions of swellable nacreous walls

The maintenance of open, unobstructed sieve element lumina represents a structural optimization of the sieve tube network for rapid mass flow. The constriction of sieve tubes by nacreous walls clearly reduces the transport efficiency of the system. Nonetheless, swellable nacreous walls could improve the overall functionality of the network by various mechanisms.

If the hydration-dependent expansion of nacreous walls is limited by the compressive force that the protoplast exerts on the wall as hypothesized above, the swelling state of the wall will change with turgor changes as long as turgor remains below the value required for maximum wall compression. Above that turgor threshold, the cross-sectional area of the sieve tube lumen will be at its maximum, allowing for maximum transport rates. Decreasing turgor pressure below the threshold will allow the wall to take up water and swell, and increasing turgor will drive water out of the wall again and make it shrink. Such interactions between turgor and wall swelling would have two important biomechanical consequences. First, fluctuations of turgor pressure in the protoplast would be buffered by the expansive tendencies of the wall. In sieve tubes, this turgor buffering could stabilize the pressure gradient that drives pressure flow during periods in which the plant is stressed and unable to maintain constant high turgor. Second, a separation of the protoplast from the inner surface of the wall, or plasmolysis, will be prevented by wall swelling, even if the protoplast suffers dramatic volume loss. Therefore, swellable walls could minimize damage to plasmodesmata (Oparka, 1994) and other structurally and developmentally important links between the wall and the plasma membrane (McKenna *et al.*, 2014; Liu *et al.*, 2015) under conditions of severe osmotic and water stress. The observation that sieve elements with swollen nacreous walls retain channels that connect to plasmodesmata in cell wall pits (Figure 5) is in line with this interpretation.

Nacreous walls constrict sieve elements efficiently (Figures 4 and 5), which might represent a physiological function in itself. So far, two experimentally verified mechanisms of physiologically regulated, reversible sieve tube occlusion are known. First, callose depositions control sieve plate conductivity and enable the temporary closure of sieve tubes during periods of dormancy (Eschrich, 1975; Levy and Epel, 2009). Callose deposition on sieve plates can be induced by wounding and biotic as well as abiotic stresses (Sjölund, 1997; Levy and Epel, 2009; Nalam *et al.*, 2019), but the process is too slow to create an immediate occlusion (Mullendore *et al.*, 2010). Second, protein bodies called forisomes are capable of blocking flow in sieve element-sized artificial microtubes due to their Ca^{2+}-dependent contractility, and may do the same in real sieve tubes (Knoblauch *et al.*, 2012). This mechanism lacks general significance, though, as forisomes are restricted to the Papilionoids in the legume family (Fabaceae s.l.; Peters *et al.*, 2010). P-proteins other than the forisome-forming SEO family have been postulated to prevent assimilate loss by sealing wounded sieve tubes (Fischer, 1885; Ernst *et al.*, 2012), but available evidence concerning this idea is inconclusive (Knoblauch *et al.*, 2014; see also Sabnis and Sabnis, 1995). We note that swellable nacreous walls would add a particularly efficient emergency shutdown mechanism to this repertoire, as they activate automatically, immediately, and possibly reversibly when sieve elements experience wounding-induced or pathogen-induced drops in turgor.

To conclude, we have demonstrated that nacreous walls are artefacts resulting from tissue wounding during preparation for microscopy in *G. macrorhizus*. The striking structural similarity between nacreous walls in our study species and those reported from numerous other taxa suggests general applicability of our findings. *In situ*, nacreous walls form rapidly in response to sieve tube wounding. It will be interesting to see whether wall swelling in land plant sieve elements is reversible *in vivo* as it is in kelp, because this would allow swellable walls to function in turgor regulation and in wounding and defence responses.

EXPERIMENTAL PROCEDURES

Plant material

Gerrardanthus macrorhizus Harv. ex Benth. & Hook.f. 1867 from southern Africa is a climber of caudiciform habit. Vines grow from

a perennial, bulbous above-ground caudex and can be removed for experimentation without having to sacrifice the plant. Three individuals were permanently maintained in a greenhouse at the instructional plant collection of the School of Biological Sciences, Washington State University. At the time this study took place, the caudices of these experimental plants had diameters between 10 and 13 cm.

Light microscopy

A Leica SP8 CLSM equipped with white light laser and a pulser 405 nm diode laser (Leica Microsystems, Wetzlar, Germany) was used. Emission was detected with hybrid detectors. For simultaneous calcofluor white (CFW; Fluka solution 18909, Honeywell, Charlotte, NC, USA) and carboxyfluorescein diacetate (CFDA; Sigma-Aldrich, St. Louis, MA, USA) imaging, CFW was excited at 405 nm and emission was detected at 412–464 nm. CFDA was excited at 496 nm and detected at 501–598 nm. For simultaneous imaging of CFW and aniline blue (AB; Electron Microscopy Sciences, Hatfield, PA, USA), both dyes were excited at 405 nm. CFW emission was detected at 418–468 nm and AB at 550–622. Although the two dyes have partly overlapping spectra, the very broad emission spectrum of AB allows separate detection of the dye in the yellow to orange range.

For *in situ* confocal microscopy, paradermal slices were cut off the main vein of leaves connected to the live plant to expose intact sieve tubes (Knoblauch and van Bel, 1998). The cells exposed in this observation window were covered in 10 mM KCl, 10 mM NaCl, and 0.2 mM EDTA. CFW solution was applied in this medium at a ratio of 1:30. CFDA was dissolved at 10 mg ml^{-1} in 100% acetone. Ten μl of this CFDA stock per ml distilled water were injected into the leaves, by pushing the solution through stomata with a syringe at a position several centimetres upstream of the observation window.

For simultaneous AB and CFW imaging of hand sections, the dyes were applied in a mixture of 0.01% AB and 1% of Fluka CFW solution in 10 mM *N*-cyclohexyl-2-aminoethanesulfonic acid (CHES) buffer at pH 10.

For *in situ* manipulations of transporting sieve elements, microcapillaries with a tip diameter of about 1 μm were pulled from borosilicate glass on a Sutter Instruments (Novato, CA, USA) model P-2000 micropipette puller. Experiments were conducted on the Leica SP-8 confocal microscope equipped with a Sutter Instruments manipulator model MP-285.

Electron microscopy

For transmission electron microscopy, samples were fixed in 4% glutaraldehyde in 0.05 M cacodylate buffer for 2 h and then further fixed in a microwave oven (Biowave Pro, Pelco, CA, USA) at 300 W for 2 min at a maximum temperature of 40°C. The samples were post-fixed in 2% osmium tetroxide over night at 4°C and then dehydrated in acetone in 10% increments from 10 to 90% in a microwave oven for 1 min each at 750 W with a temperature maximum of 35°C followed by a 2 min rest. Dehydration was finalized by three periods of 10 min each in 100% dried acetone at room temperature. The samples were resin-infiltrated in acetone-resin mixtures at ratios of 3:1, 2:1, 1:1, 1:2, 1:3, and twice in pure resin for 8 h each, and then polymerized in an oven at 65°C for 24 h. The samples were cut using a Leica M 80 ultramicrotome (Leica Microsystems, Wetzlar, Germany) and observed using an FEI T-20 TEM; FEI, Hillsboro, OR, USA).

Image analysis

Analyses of micrographs including determinations of cell sizes, cross-sectional areas, and volumes as well as manipulations of image stacks for 3D reconstructions and optical sectioning were performed using the free open-source software FIJI (ImageJ 2.0.0-rc-69/1.52p; https://imagej.nih.gov/ij/). Visualizations of 3D structural information of entire sieve elements were produced with the free open-source software MeshLab v2016.12 (http://www.meshlab.net/).

ACKNOWLEDGEMENTS

We thank Chuck Cody for obtaining and maintaining the experimental plants, and the Franceschi Microscopy and Imaging Center (WSU) for technical support. This work was supported by the US National Science Foundation (grant number 1656769).

AUTHOR CONTRIBUTIONS

MK and WSP developed the project. MK designed and coordinated the experimental work, which was conducted by JK and VV. WSP performed quantitative data analyses and wrote the manuscript with input from all authors.

CONFLICT OF INTEREST

The authors declare no conflict of interest.

DATA AVAILABILITY STATEMENT

All relevant data can be found within the manuscript and its supporting materials. All original data (confocal and electron micrographs) produced for this study are available from the corresponding author upon request.

SUPPORTING INFORMATION

Additional Supporting Information may be found in the online version of this article.

Table S1. Reported distribution of nacreous walls in land plants, compiled from literature dating from 1900 onwards.

Figure S1. Reported distribution of nacreous walls in angiosperms, plotted onto angiosperm phylogeny.

REFERENCES

Behnke, H.D. (1971) Über den Feinbau verdickter (nacré) Wände und der Plastiden in den Siebröhren von *Annona* und *Myristica*. *Protoplasma*, **72**, 69–78.

Behnke, H.D. and Sjolund, R.D. (1990) *Sieve Elements*. Berlin, Germany: Springer.

Biebl, R. (1938) Trockenresistenz und osmotische Empfindlichkeit der Meeresalgen verschieden tiefer Standorte. *Jahrb. Wiss. Bot.* **86**, 350–386.

Botha, C.E.J. and Evert, R.F. (1981) Studies on *Artemisia afra* Jacq.: the phloem in stem and leaf. *Protoplasma*, **109**, 217–231.

Bourquin, V., Nishikubo, N., Abe, H., Brumer, H., Denman, S., Eklund, M., Christiernin, M., Teeri, T.T., Sundberg, B. and Mellerowicz, E.J. (2002) Xyloglucan endotransglycosylases have a function during the formation of secondary cell walls of vascular tissues. *Plant Cell*, **14**, 3073–3088.

Boutté, Y., Vernhettes, S. and Satiat-Jeunemaitre, B. (2007) Involvement of the cytoskeleton in the secretory pathway and plasma membrane organisation of higher plant cells. *Cell Biol. Int.* **31**, 649–654.

Buwalda, S.J., Boere, K.W.M., Dijkstra, P.J., Feijen, J., Vermonden, T. and Hennink, W.E. (2014) Hydrogels in a historical perspective: from simple networks to smart materials. *J. Contr. Release*, **190**, 254–273.

Carpita, N.C. (2012) Progress in the biological synthesis of the plant cell wall: new ideas for improving biomass for bioenergy. *Curr. Opin. Biotechnol.* **23**, 330–337.

Chafe, S.C. and Doohan, M.E. (1972) Observations on the ultrastructure of the thickened sieve cell wall in *Pinus strobus* L. *Protoplasma*, **75**, 67–78.

Chang, C.Y. (1935) Differentiation of protophloem in the angiosperm shoot. *New Phytol.* **34**, 21–29.

Cheadle, V.I. and Esau, K. (1958) Secondary phloem of Calycanthaceae. *Univ. Calif. Publ. Bot.* **29**, 397–509.

Cronshaw, J. (1975) Sieve element cell walls. In *Phloem Transport* (Aronoff, S., Dainty, J., Gorham, P.R., Srivastava, L.M. and Swanson, C.A., eds). New York: Plenum Press, pp. 129–147.

Douglas, F.F., Gasiorek, J.M. and Swaffield, J.A. (1995) *Fluid Mechanics*, 3rd edn. Harlow, UK: Longman Scientific & Technical.

Ehlers, K., Knoblauch, M. and van Bel, A.J.E. (2000) Ultrastructural features of well-preserved and injured sieve elements: minute clamps keep the phloem conduits free for mass flow. *Protoplasma*, **214**, 80–92.

Ernst, A.M., Jekat, S.B., Zielonka, S., Müller, B., Neumann, U., Rüping, B., Krzyzanek, V., Prüfer, D. and Noll, G.A. (2012) Sieve element occlusion (SEO) genes encode structural phloem proteins involved in wound sealing of the phloem. *Proc. Natl Acad. Sci. USA*, **109**, E1980–E1989.

Esau, K. (1938) Ontogeny and structure of the phloem of tobacco. *Hilgardia*, **11**, 343–424.

Esau, K. (1939) Development and structure of the phloem tissue. *Bot. Rev.* **5**, 373–432.

Esau, K. (1969) The Phloem. In *Encyclopedia of Plant Anatomy*, Vol. 5 Part 2. Berlin, Germany: Gebrüder Borntraeger.

Esau, K. and Cheadle, V.I. (1958) Wall thickening in sieve elements. *Proc. Natl Acad. Sci. USA*, **44**, 546–553.

Eschrich, W. (1975) Sealing systems in phloem. In *Phloem Transport (Encyclopedia of Plant Physiology. New Series, vol. 1. Transport in Plants)* (Zimmermannn, M.H. and Milburn, J.A. eds). Berlin, Germany: Springer, pp. 39–56.

Evert, R.F. (1963) Ontogeny and structure of the secondary phloem in *Pyrus malus*. *Am. J. Bot.*, **50**, 8–37.

Evert, R.F. (1982) Sieve-tube structure in relation to function. *Bio-Science*, **32**, 789–795.

Evert, R.F. (1990) Dicotyledons. In *Sieve Elements* (Behnke, H.D. and Sjolund, R.D., eds). Berlin, Germany: Springer, pp. 103–137.

Evert, R.F. and Eichhorn, S.E. (1976) Sieve-element ultrastructure in *Platycerium bifurcatum* and some other polypodiaceous ferns: the nacreous wall thickening and maturation of the protoplast. *Am. J. Bot.* **63**, 30–48.

Evert, R.F., Eschrich, W. and Heyser, W. (1978) Leaf structure in relation to solute transport and phloem loading in *Zea mays* L. *Planta*, **138**, 279–294.

Fischer, A. (1885) Ueber den Inhalt der Siebröhren in der unverletzten Pflanze. *Ber. Deut. Bot. Ges.* **3**, 230–239.

Froelich, D.R., Mullendore, D.L., Jensen, K.H., Ross-Elliott, T.J., Anstead, J.A., Thompson, G.A., Pélissier, H.C. and Knoblauch, M. (2011) Phloem ultrastructure and pressure flow: sieve-element-occlusion-related agglomerations do not affect translocation. *Plant Cell*, **23**, 4428–4445.

Furch, A.C.U., Zimmermann, M.R., Will, T., Hafke, J.B. and van Bel, A.J.E. (2010) Remote-controlled stop of phloem mass flow by biphasic occlusion in *Cucurbita maxima*. *J. Exp. Bot.* **61**, 3697–3708.

Gilliland, M.G., van Staden, J. and Bruton, A.G. (1984) Studies on the translocation system of guayule (*Parthenium argentatum* Gray). *Protoplasma*, **122**, 169–177.

Heo, J.O., Blob, B. and Helariutta, Y. (2017) Differentiation of conductive cells: a matter of life and death. *Curr. Opin. Plant Biol.* **53**, 23–29.

Holzinger, A., Herburger, K., Kaplan, F. and Lewis, L.A. (2015) Desiccation tolerance in the charophyte green alga *Ulva compressa*: does cell wall architecture contribute to ecological success? *Planta*, **242**, 477–492.

Israel, H.W., McGovern, R.J. and Horst, R.K. (1992) Chrysanthemum phloem necrosis: onset of systemic ultrastructural changes. *Int. J. Plant Sci.* **153**, 197–204.

Karsten, U. (2012) Seaweed acclimation to salinity and desiccation stress. In *Seaweed Biology (Ecological Studies 219)* (Wiencke, C. and Bischoff, K., eds). Berlin, Germany: Springer, pp. 87–107.

Kim, S.J. and Brandizzi, F. (2016) The plant secretory pathway for the trafficking of cell wall polysaccharides and glycoproteins. *Glycobiology*, **29**, 940–949.

Knoblauch, M. and Peters, W.S. (2010) Münch, morphology, microfluidics – our structural problem with the phloem. *Plant Cell Environ.* **33**, 1439–1452.

Knoblauch, M. and Peters, W.S. (2013) Long-distance translocation of photosynthates: a primer. *Photosynth. Res.* **117**, 189–196.

Knoblauch, M. and Peters, W.S. (2017a) Symplasmic mass flow and sieve tubes in algae and plants. *Perspect. Phycol.* **4**, 93–101.

Knoblauch, M. and Peters, W.S. (2017b) What actually is the Münch hypothesis? A short history of assimilate transport by mass flow. *J. Integr. Plant Biol.* **59**, 292–310.

Knoblauch, M. and van Bel, A.J.E. (1998) Sieve tubes in action. *Plant Cell*, **10**, 35–50.

Knoblauch, M., Stubenrauch, M., van Bel, A.J.E. and Peters, W.S. (2012) Forisome performance in artificial sieve tubes. *Plant Cell Environ.* **35**, 1419–1427.

Knoblauch, M., Froelich, D.R., Pickard, W.F. and Peters, W.S. (2014) SEORious business: structural proteins in sieve tubes and their involvement in sieve tube occlusion. *J. Exp. Bot.* **65**, 1879–1893.

Knoblauch, J., Peters, W.S. and Knoblauch, M. (2016a) The gelatinous extracellular matrix facilitates transport studies in kelp: visualization of pressure-induced flow reversal across sieve plates. *Ann. Bot.* **117**, 599–606.

Knoblauch, J., Tepler Drobnitch, S., Peters, W.S. and Knoblauch, M. (2016b) *In situ* microscopy reveals reversible cell wall swelling in kelp sieve tubes: one mechanism for turgor generation and flow control? *Plant Cell Environ.* **39**, 1727–1736.

Knoblauch, M., Knoblauch, J., Mullendore, D.L., Savage, J.A., Babst, B.A., Beecher, S.D., Dodgen, A.C., Jensen, K.H. and Holbrook, N.M. (2016c) Testing the Münch hypothesis of long distance phloem transport in plants. *eLife*, **5**, 315341.

Kopeček, J. (2007) Hydrogel biomaterials: a smart future? *Biomaterials*, **28**, 5185–5192.

Kotte, H. (1915) Turgor und Membranquellung bei Meeresalgen. *Wiss. Meeresunters. (Abt. Kiel)*, **23**, 115–167.

Kuo, J. (1983) The nacreous walls of sieve elements in seagrasses. *Am. J. Bot.* **70**, 159–164.

Kuo, J. and Stewart, J.G. (1995) Leaf anatomy and ultrastructure of the North American marine angiosperm *Phyllospadix* (Zosteraceae). *Can. J. Bot.* **73**, 827–842.

Levy, A. and Epel, B.L. (2009)Cytology of the (1–3)-β-glucan (callose) in plasmodesmata and sieve plate pores. In *Chemistry, Biochemistry, and Biology of (1→3)-β-Glucans and related Polysaccharides* (Bacic, A., Fincher, G.B. and Stone, B.A., eds). Burlington, USA: Academic Press, pp. 439–463.

Liu, Z., Persson, S. and Sánchez-Rodríguez, C. (2015) At the border: the plasma membrane-cell wall continuum. *J. Exp. Bot.* **66**, 1553–1563.

Lough, T.J. and Lucas, W.J. (2006) Integrative plant biology: role of phloem long-distance macromolecular trafficking. *Annu. Rev. Plant Biol.* **57**, 203–232.

Machado, S.R. and Sajo, M.G. (1996) Occurrence of form Pllcf sieve-element plastids in *Xyris* species (Xyridaceae). *Ann. Bot.* **78**, 671–673.

de Marco, F., Pagliari, L., Degola, F., Buxa, S.V., Loschi, A., Dinant, S., Le Hir, R., Morin, H., Santi, S. and Musetti, R. (2016) Combined microscopy and molecular analyses show phloem occlusions and cell wall modifications in tomato leaves in response to '*Candidatus* Phytoplasma solani'. *J. Microsc.* **263**, 212–225.

de Schepper, V., de Swaef, T., Bauweraerts, I. and Steppe, K. (2013) Phloem transport: a review of mechanics and control. *J. Exp. Bot.* **64**, 4839–4850.

McKenna, J.F., Tolmie, A.F. and Runions, J. (2014) Across the great divide: the plant cell surface continuum. *Curr. Opin. Plant Biol.* **22**, 132–140.

Mehta, A.S. and Spanner, D.C. (1962) The fine structure of the sieve tubes of the petiole of Nymphoides peltatum (Gmel.) O. Kunze. *Ann. Bot.* **26** (N.S.), 291–299.

Mostaert, A.S. and King, R.J. (1993) The cell wall of the halotolerant red alga *Caloglossa leprieurii* (Montagne) J. Agardh (Ceramiales, Rhodophyta) from freshwater and marine habitats: effect of changing salinity. *Cryptogam. Bot.* **4**, 40–46.

Mostaert, A.S., Karsten, U. and King, R.J. (1995) Inorganic ions and mannitol in the red alga *Caloglossa leprieurii* (Ceramiales, Rhodophyta): response to salinity change. *Phycologia*, **34**, 501–507.

Mullendore, D.L., Windt, C.W., van As, H. and Knoblauch, M. (2010) Sieve tube geometry in relation to phloem flow. *Plant Cell*, **22**, 579–593.

Münch, E. (1930) *Die Stoffbewegungen in der Pflanze*. Jena, Germany: Gustav Fischer.

Nalam, V., Louis, J. and Shah, J. (2019) Plant defense against aphids, the pest extraordinaire. *Plant Sci.* **279**, 96–107.

Nii, N., Hase, K. and Uchida, H. (1994) Anatomical features on the sieve elements and sorbitol content in various organs of Rosaceae fruit trees. *J. Jpn. Soc. Hortic. Sci.* **62**, 739–747.

Oparka, K.J. (1994) Plasmolysis: new insights into an old process. *New Phytol.* **126**, 571–591.

Oparka, K.J., Duckett, C.M., Prior, D.A.M. and Fisher, D.B. (1994) Real-time imaging of phloem-unloading in the root tip of *Arabidopsis*. *Plant J.* **6**, 759–66.

Peters, W.S., Haffer, D., Hanakam, C.B., van Bel, A.J.E. and Knoblauch, M. (2010) Legume phylogeny and the evolution of a unique contractile apparatus that regulates phloem transport. *Am. J. Bot.* **97**, 797–808.

Sabnis, D.D. and Sabnis, H.M. (1995) Phloem proteins: structure, biochemistry and function. In *The Cambial Derivatives (Encyclopedia of Plant Anatomy, Vol. 9 Part 4)* (Iqbal, M., ed). Berlin, Germany: Gebrüder Borntraeger, pp. 271–292.

Savage, J.A., Clearwater, M.J., Haines, D.F., Klein, T., Mencuccini, M., Sevanto, S., Turgeon, R. and Zhang, C. (2016) Allocation, stress tolerance and carbon transport in plants: how does phloem physiology affect plant ecology? *Plant, Cell Environ.* **39**, 709–725.

Schlag, M.G. and Gal, M. (1996) The nacreous sieve-element wall in healthy and in MLO-infected apple trees. *Intern. J. Plant Sci.* **157**, 80–91.

Schmidt, E.W. (1917) *Bau und Funktion der Siebröhre der Angiospermen*. Jena, Germany: Gustav Fischer.

Schmitz, K. (1990) Algae. In *Sieve Elements* (Behnke, H. D. and Sjolund, R. D., eds). Berlin, Germany: Springer, pp. 1–18.

Schmitz, K. and Srivastava, L.M. (1974) Fine structure and development of sieve tubes in *Laminaria groenlandica* Rosenv. *Cytobiologie*, **10**, 66–87.

Sjölund, R.D. (1997) The phloem sieve element: a river runs through it. *Plant Cell*, **9**, 1137–1146.

Sterling, C. (1946) Growth and vascular development in the shoot apex of *Sequoia sempervirens* (Lamb.) Endl. III. Cytological aspects of vascularization. *Am. J. Bot.* **33**, 35–45.

Stevenson, D.W. (1977) Histochemical and ultrastructural observations on the nacreous walls of the sieve elements of *Atrichum undulatum*. *Ann. Bot.* **41**, 849–853.

Sykes, M.G. (1908) Anatomy and histology of *Macrocystis pyrifera* and *Laminaria saccharina*. *Ann. Bot.* **22**, 291–325.

Torode, T.A., O'Neill, R., Marcus, S.E. *et al.* (2018) Branched pectic galactan in phloem-sieve-element cell walls: implications for cell mechanics. *Plant Physiol.* **176**, 1547–1558.

Truernit, E. (2014) Phloem imaging. *J. Exp. Bot.* **65**, 1881–1688.

Walter, H. and Kreeb, K. (1970) *Die Hydratation und Hydratur des Protoplasmas der Pflanzen und ihre öko-physiologische Bedeutung (Protoplasmatologia, Vol. II C 6)*. Vienna, Austria: Springer.

van Went, J.L. and Tammes, P.M.L. (1973) Trumpet filaments in *Laminaria digitata* as an artefact. *Acta Bot. Neerl.* **22**, 112–119.

Zimmermann, A. (1922) *Die Cucurbitaceen*. Jena, Germany: Gustav Fischer.